RANDOM MUTAGENESIS OF PRESENILIN 1 IDENTIFIES NOVEL MUTANTS EXCLUSIVELY GENERATING LONG AMYLOID β PEPTIDES*

Yoshifumi Nakaya‡§, Takuya Yamane‡, Hirohisa Shiraishi¶, Hua-Qin Wang‡, Etsuro Matsubara||, Toru Sato, Georgia Dolios††, Rong Wang††, Bart De Strooper‡‡, Mikio Shoji||, Hiroto Komano¶, Katsuhiko Yanagisawa¶, Yasuo Ihara**, Paul Fraser§§, Peter St George-Hyslop§§, and Masaki Nishimura‡**

From the ‡Molecular Neuroscience Research Center, Shiga University of Medical Science, Shiga 520-2192, the §Department of Neurology, Kyoto University Graduate School of Medicine, Kyoto 606-8507, the ¶Department of Dementia Research, National Institute for Longevity Sciences, Aichi 474-8522, the ||Department of Neurology, Okayama University Graduate School of Medicine and Density, Okayama 700-8558, **Department of Neuropathology, Faculty of Medicine, University of Tokyo, Tokyo 113-0033, Japan, the ††Department of Human Genetics, Mount Sinai School of Medicine, New York, NY 10029, the ‡‡Center for Human Genetics, K.U. Leuven and Flanders Interuniversity Institute for Biotechnology, 3000 Leuven, Belgium, and the §§Centre for Research in Neurodegenerative Diseases, University of Toronto, Toronto, Ontario M5S 3H2, Canada

Running Title: PS1 mutations causing exclusive generation of long Aβ

Address correspondence to: Masaki Nishimura, Molecular Neuroscience Research Center, Shiga University of Medical Science, Seta, Otsu, Shiga 520-2192, Japan. Tel.: 81-77-548-2327; Fax: 81-77-548-2402; E-mail: mnishimu@belle.shiga-med.ac.jp.

Familial Alzheimer's disease-causing mutations in the presenilins increase production of longer, pathogenic amyloid β peptides ($A\beta_{42/43}$) by altering γ-secretase activity. The mechanism underlying this effect remains unknown, although it has been proposed that heteromeric macromolecular complexes containing presenilins mediate γ-secretase cleavage of the amyloid β precursor protein. Using a random mutagenesis screen of presenilin 1 (PS1) for PS1-endoproteolysis-impairing mutations, we identified five unique mutants including R278I- and L435H-PS1, which exclusively generated a high level of $A\beta_{43}$ but that did not support physiological PS1 endoproteolysis or $A\beta_{40}$ generation. These mutants did not measurably alter the molecular size or subcellular localization of PS1 complexes. Pharmacological studies indicated that the upregulation of activity for $A\beta_{43}$ generation by these mutations was not further enhanced by the difluoroketone inhibitor DFK167 and was refractory to inhibition by sulindac sulfide. These results suggest that PS1 mutations can lead to a wide spectrum of changes in the activity and specificity of γ-secretase and that the effects of PS1 mutations and γ-secretase inhibitors on the specificity are mediated through a common mechanism.

The amyloid β-precursor protein (APP)[1], Notch, ErbB-4, and several other unrelated type 1 transmembrane (TM) proteins undergo γ-secretase cleavage within their TM domains (1, 2). The consequential proteolytic release of intracellular domains of these substrates has been revealed to be involved in signaling from the membrane to the nucleus (3). In the case of APP, γ-secretase mediates γ- and ε-cleavage to generate a

heterogeneous series of N- and C-terminal products, named amyloid β peptides (Aβ) and APP intracellular domain (AICD), respectively. Aβ peptides have C-termini that end at residues 38, 40, 42, or 43, while AICD fragments begin at residues 48 to 52 of the Aβ peptide domain (4, 5). The process regulating these heterogeneous intramembranous cleavages is poorly understood but is a central issue in Alzheimer's disease (AD) research for three reasons. First, the longer Aβ species ending at residue 42 or 43 ($Aβ_{42/43}$) are thought to play a critical role in the pathogenesis of AD, although they are minor products of normal γ-secretase activity (6). Second, clinical mutations in the presenilins (PSs), which are responsible to the majority of familial AD (FAD) pedigrees, cause increased ratio of $Aβ_{42/43}$ isoforms to total Aβ (7). Third, medication that modulates the $Aβ_{42/43}$ production by altering γ-secretase activity could provide an effective therapy for AD.

Presenilin 1 and 2 (PS1 and PS2) are multi-pass TM proteins and undergo endoproteolysis within their large cytoplasmic loop domains by an unknown protease named presenilinase (PSase) (8, 9). This endoproteolysis yields N- and C-terminal fragments (NTF and CTF, respectively) that are stabilized and assembled into functional macromolecular complexes together with at least three other membrane proteins, nicastrin (Nct), APH-1 and PEN-2 (10, 11). The abundance and stoichiometry of PS complexes are tightly regulated, and exogenously over-expressed PSs can replace endogenous PSs (8). Recent studies have suggested that these multiprotein complexes mediate γ-secretase cleavage and probably PS endoproteolysis and that PSs may be the catalytic components of the complexes (2, 12-15). Furthermore, it has been presumed that FAD-associated mutations of the PSs significantly alter γ-secretase activity and enhance production of $Aβ_{42/43}$ through a gain-of-function effect. However, it is still unclear how more than a hundred of FAD-linked missense mutations scattered throughout the sequence of PSs can selectively upregulate the enzymatic production of $Aβ_{42/43}$.

While trying to address this conundrum, we realized that the FAD-linked mutations and the few site-directed mutagenesis studies described to date (12, 16-19) did not provide an unbiased view of the effects of PS mutations on γ-secretase activity. Thus, the clinical mutations were ascertained by linkage to FAD, whereas the site-directed mutations in conserved residues were created to test specific hypotheses. We therefore undertook a screen of randomly mutagenized PS1 to identify single-residue missense mutations that affected the physiological endoproteolysis of PS1 and/or selectively changed Aβ isoform production. We report here the discovery and characterization of novel mutant PS1 that exclusively generate longer Aβ species, but which do not support the activities for $Aβ_{40}$ generation or PS1 endoproteolysis.

EXPERIMENTAL PROCEDURES

Antibodies and reagents - The rabbit polyclonal antibody against the N-terminus of PS1 was previously described (10). Monoclonal antibodies against PS1 CTF and APP NTF (22C11) and a polyclonal antibody against APP CTF were purchased from Chemicon (Temecula, CA). Polyclonal anti-nicastrin (N1660) and monoclonal anti-Flag tag (M2) antibodies were from Sigma (St. Louis, MO). Monoclonal antibodies against p115 and Myc tag (9E10) were obtained from BD Biosciences (Franklin Lakes,

NJ) and Santa Cruz Biotechnology (Santa Cruz, CA), respectively. Cycloheximide, DFK167 and sulindac sulfide were purchased from Sigma, Enzyme Systems Products (Livermore, CA) and Wako (Osaka, Japan), respectively.

Cell culture and cDNA transfection - Human embryonic kidney 293 (HEK293) cells and mouse embryonic fibroblasts derived from PS1-, PS2-double knock-out mouse (PS-null MEFs) (20) were cultured in Dulbecco's modified Eagle medium supplemented with 10% fetal bovine serum and 1% streptomycin/penicillin. cDNA transfection was carried out using LipofectAMINE Plus reagent (Invitrogen, Carlsbad, CA).

Generation and screening of a randomly mutagenized PS1 cDNA library - Random mutagenesis of PS1 cDNA was performed by error-prone PCR with the forward primer 5'-TTTTGAATTCTCCTTAGACAGCTTGGCC TGGAG-3', corresponding to the 5'-untranslated region of human PS1 cDNA and containing an *EcoR*I restriction site; and with the reverse primer 5'-TTTTCTCGAGACCTTTGTCCTCCCCAGA TTTGG-3', corresponding to the 3'-untranslated region and containing an *Xho*I site. PCR conditions were determined for low frequency mutagenesis according to the manufacturer's instructions (Stratagene, La Jolla, CA). By sequencing 10 PCR products, we confirmed that the number of nucleotide substitutions per PS1 cDNA ranged from zero to seven. Mutagenized PS1 cDNA fragments obtained from four different PCR reactions were cloned into the *EcoR*I/*Xho*I sites of pCMV-script (Stratagene). Site-directed mutagenesis for subsequent confirmatory experiments was carried out using the QuikChange mutagenesis kit (Stratagene) and appropriate synthesized oligonucleotide primers. For screening for endoproteolysis-impaired mutants, PS-null MEFs were transfected with each mutagenized PS1 cDNA. At 48 h after transfection, cells were harvested and homogenized in a Teflon-glass homogenizer. Crude membrane fractions were isolated from the postnuclear supernatants by centrifugation at 12,000*g* for 30 min and then subjected to Western analysis with an antibody against PS1.

Retrovirus-mediated gene expression - The retroviral infection of PS-null MEFs was carried out as described (21). Briefly, PLATE-E packaging cells were transfected with a retroviral vector, pMXs, carrying the cDNA encoding PS1 or human APP using FuGene-6 (Roche Diagnostics). Culture media collected two days after transfection were used for viral stocks. For infection, MEFs were incubated with virus stock containing 10 μg/ml Polybrene (Sigma) for 6 h. A day after infection, the medium was replaced with fresh Dulbecco's modified Eagle medium supplemented with 10% fetal bovine serum and 1% streptomycin/penicillin, and the MEFs were cultured for another 48 h for the preparation of conditioned media to be used in Aβ measurements. The infection efficiency was more than 95% in this study, estimated by a control experiment using pMXs-GFP that carried cDNA for jellyfish green fluorescent protein.

Immunoprecipitation and Western analysis - Cells or membrane fractions were lysed in lysis buffer (25 mM HEPES at pH 7.5, 150 mM NaCl, 2 mM EDTA and 10% glycerol) containing 1% NP40 and protease inhibitor cocktail (Roche Diagnostics). Western blotting was performed as previously described (10). For immunoprecipitation, cells were lysed in lysis buffer containing 1% 3-[(3-cholamidopropyl)dimethylammonio]-2-hydr oxy-1-propanesulfonic acid (CHAPSO). After preclearing with protein A-Sepharose CL-4B

(Amersham Biosciences, Uppsla, Sweden), cell lysates were incubated with antibody for 2 h, followed by overnight incubation with protein A-Sepharose at 4ºC. The immunoprecipitates were washed three times with 1% CHAPSO buffer and analyzed by Western blotting.

Glycerol velocity gradient centrifugation - Glycerol velocity gradient centrifugation was carried out as previously described (22). HEK293 cells transfected with PS1 cDNA were disrupted with a Polytron homogenizer (Kinematica, Littau-Luzern, Switzerland), and nuclei and large cell debris were sedimented by centrifugation at 1,500 *g* for 10 min. The postnuclear supernatants were centrifuged at 100,000 *g* for 1 h in a Beckman ultracentrifuge to prepare crude membrane fractions. After solubilization in lysis buffer containing 1% CHAPSO, membrane fractions were applied onto the top of 15 to 30% (w/v) linear glycerol gradients. The gradients were centrifuged at 36,000 *g* for 18 h and split into 12 fractions from the bottom. The fractionated proteins were analyzed by Western blotting. Ferritin (440 kDa), β amylase (200 kDa), lactate dehydrogenase (140 kDa) and bovine serum albumin (67 kDa) are used as molecular weight markers.

Evaluation of PS-dependent cleavages of APP and Notch - For analysis of AICD generation, crude membrane fractions were obtained from HEK293 cells expressing various PS1 mutants and were solubilized in lysis buffer containing 0.5% CHAPSO and 5 mM 1,10-phenanthroline (Sigma). The lysates were incubated for 1 h at 37ºC and analyzed by Western blotting. For assessment of Notch intracellular domain (NICD) generation, HEK293 cells expressing the PS1 mutant were transiently transfected with NotchΔE tagged with Myc epitopes (23). After starvation in Met-free medium, cells were metabolically labeled for 20 min with 500 μCu/ml ^{35}S-Met (ICN Biomedicals) and then incubated for 1 h in complete Dulbecco's modified Eagle medium supplemented with 10% fetal bovine serum. Cell lysates were immunoprecipitated with anti-Myc antibody and separated by polyacrylamide gel electrophoresis. Secreted Aβ levels were measured by enzyme-linked immunosorbent assays (ELISAs) specific for $A\beta_{40}$ or $A\beta_{42/43}$ as described (24).

Immunoprecipitation/mass spectrometry analysis - Immunoprecipitation/mass spectrometry (IP/MS) analysis of Aβ peptides was performed as previously described (4). Secreted Aβ peptides in conditioned media were immunoprecipitated with the monoclonal antibody 4G8 (Senetek, Napa, CA) using Protein A/G-Plus agarose beads (Santa Cruz Biotechnology). Aβ peptides were analyzed by matrix-assisted laser desorption/ionization time-of-flight mass spectrometry (MALDI-TOF-MS) using a Voyager-DE STR mass spectrometer (Applied Biosystems, Foster City, CA). Each mass spectrum was averaged from 1,000 measurements and calibrated with bovine insulin as an internal calibrant.

Immunocytochemistry - Cells were fixed with 4% paraformaldehyde for 15 min and were then permeabilized with 0.1% Triton X-100 for 5 min. Nonspecific antibody binding was blocked by incubating cells with 5% normal goat serum for 1 h. For double staining, fixed cells were incubated overnight at 4°C with a mixture of primary antibodies, followed by reaction for 2 h with Alexa Fluor 594-conjugated anti-rabbit and Alexa Fluor 488-conjugated anti-mouse secondary antibodies (Molecular Probes). The slides were analyzed with an LSM510 confocal laser-scanning microscope (Carl Zeiss, Oberkochen, Germany).

Subcellular fractionation with discontinuous sucrose gradients - Subcellular fractionation was performed according to a previously described method (22). HEK293 cells transfected with PS1 cDNA were homogenized with a Polytron homogenizer in a buffer (5 mM HEPES at pH 7.2, 1 mM EDTA and protease inhibitor cocktail). Postnuclear supernatant was obtained by centrifugation at 1,000 *g* for 10 min and loaded on the top of a discontinuous sucrose gradient (1 ml/2.0 M, 3.4 ml/1.3 M, 3.4 ml/1.0 M and 2.7 ml/0.6 M) made up in the same buffer. The gradient was centrifuged for 2 h at 280,000 *g* in a Beckman ultracentrifuge and 24 fractions were collected from the bottom of the tube with a peristaltic pump. Fractions were trichloroacetic acid-precipitated, and proteins were analyzed by Western blotting.

RESULTS

Random mutagenesis screen identified novel endoproteolysis-impaired PS1 mutants - We generated and screened a randomly mutagenized PS1 cDNA library to identify mutants that were defective in PS1 endoproteolysis. We isolated 370 clones that were then transiently transfected into PS-null MEFs. On Western analysis, 33 of the PS1 mutants displayed impaired PS1 endoproteolysis. DNA sequencing revealed that 7 of these mutants had nonsense mutations. The remaining 26 mutants harbored missense mutations that were located throughout the molecule (data not shown). Six of these 26 mutants contained single amino acid substitutions, which were S141R, T245I, R278I, P433L, A434T and L435H (Fig. 1*A* and *B*). The S141 and T245 residues are located within the second and sixth TM domains, respectively, and are not conserved in homologues of *Caenorhabditis elegans*. R278 is a conserved residue at the N-terminus of the cytoplasmic loop between TM6 and TM7; and P433, A434 and L435 are located in the highly conserved PAL motif in the cytoplasmic C-terminal tail (17).

Mutant PS1 proteins form stable, high molecular weight complexes - To assess the functional properties of these mutant PS1, each was stably transfected into HEK293 cells that also expressed a construct equivalent to the C-terminal β-secretase-processed APP fragment (C99), which is the immediate substrate for γ-secretase and yields Aβ. Because functional endoproteolytic derivatives of wild-type (WT) PS1 assemble into a stable, high molecular weight (MW) complex (22), we initially investigated: 1) the incorporation of each mutant into macromolecular complexes; 2) the ability of each mutant to replace endogenous PS1; and 3) the metabolic half-life of each mutant protein. Glycerol velocity gradient analyses revealed that the uncleaved mutant holoproteins were assembled into high MW complexes that were of similar size as the endogenous complexes (~200 to 400 kDa), although the complexes containing S141R and T245I mutants were also distributed broadly into the lower MW ranges (Fig. 1*C*). The mutant holoproteins also displaced the proteolytic fragments of endogenous presenilins (Fig. 1*C*). Reciprocal co-immunoprecipitation assays confirmed that, similar to WT-PS1, all six PS1 mutants bound to the other γ-secretase components (Nct, APH-1 and PEN-2) (data not shown). As shown in Fig. 1*D*, the half-lives of the mutant holoproteins in the presence of cycloheximide were comparable to those of WT proteolytic fragments ($t_{1/2}$ > 24 h) and were much longer than the half-life of WT holoprotein ($t_{1/2}$ < 1 h). The S141R- and T245I-PS1 holoproteins

were less well stabilized ($t_{1/2}$ = ~8 and ~4 h, respectively). Taken together, all six mutations specifically prevented PS1 endoproteolysis but did not significantly impede the assembly and stabilization of mutant PS1 complexes.

Proteolytic activities of mutant PS1 - To investigate the ability of these mutants to support γ- and ε-cleavage of APP, we measured the production of AICD and Aβ from HEK293 cell lines expressing mutant PS1 and APP-C99. In comparison to cells expressing WT-PS1, the generation of AICD was clearly suppressed in all six mutant cell lines (Fig. 2*A*). Similarly, S3 cleavage of Notch, which corresponds to ε-cleavage of APP, was clearly attenuated (Fig. 2*B*). An ELISA specific for $Aβ_{40}$ or $Aβ_{42/43}$ revealed that the levels of $Aβ_{40}$ secreted from mutant PS1-expressing cells were either comparable to or were lower than the level of $Aβ_{40}$ secreted from WT-PS1 cells (Fig. 2*C*). In contrast, the level of secreted $Aβ_{42/43}$ was significantly elevated in five of six mutant cell lines. Finally, P433L-PS1 cells secreted less $Aβ_{40}$ and $Aβ_{42/43}$ than WT-PS1 cells. These mutants exhibited dominant phenotypes for the secretion of $Aβ_{40}$ and $Aβ_{42/43}$ presumably through the replacement of endogenous PSs.

To assess the γ-secretase activity of these mutants in the absence of endogenous PSs, we transfected each of these PS1 mutants together with human APP into PS-null MEFs using retroviral vectors and then measured Aβ levels in the conditioned media from these cells (Fig. 3*A*). Transfection of WT-PS1 successfully restored Aβ secretion, whereas, compared to transfection with WT-PS1, transfection of FAD-causing mutants (I143F- and L392V-PS1) led to Aβ secretion with an increased ratio of $Aβ_{42/43}$ to total Aβ. The P433L mutant did not restore Aβ secretion, supporting the idea that P433L is a loss-of-function mutation (17, 25). In contrast, the five other mutants secreted significant amounts of $Aβ_{42/43}$, while secreting only minimal or background levels of $Aβ_{40}$. Because R278I and L435H mutants generated particularly high levels of $Aβ_{42/43}$, we focused on these mutants in the following experiments.

To reveal the profile of Aβ species secreted by MEFs expressing the R278I- or L435H-PS1, we performed IP/MS as previously described (4). The spectrum of MALDI-TOF-MS indicated that the Aβ species secreted by these MEFs always ended at residue Thr43 (i.e., $Aβ_{11-43}$ and $Aβ_{1-43}$; Fig. 3*B*). These mutants are quite unique in exclusively generating $Aβ_{43}$ and are therefore designated $PS1^{LA}$ (*PS1* yielding *l*onger *A*β).

The R278I and L435H mutations are located in the NTF and CTF of PS1, respectively (Fig. 1*B*). To determine whether these mutations might have cooperative or additive effects, we generated a PS1 cDNA harboring both mutations in *cis*. When expressed in PS-null MEFs, this double mutant formed a holoprotein that was incorporated into stable high MW complexes, but rescued neither $Aβ_{40}$ nor $Aβ_{42/43}$ secretion (data not shown). This suggests that double $PS1^{LA}$ mutation causes a loss of γ-secretase activity and that $PS1^{LA}$ are incomplete loss-of-function mutations.

PS1 endoproteolysis is thought to occur during PS1 complex maturation and prior to the activation of γ-secretase (13). To exclude the possibility that the inefficient endoproteolysis of the mutant holoproteins had affected the cleavage specificity of γ−secretase, we simulated endoproteolysis of the mutant proteins by co-infecting PS-null MEFs with two cDNAs: one encoding the PS1-NTF (residues 1 to 291), the other encoding the PS1-CTF (residues 292 to 467). In both cases, the R278I and L435H mutations

were contained in the appropriate hemi-constructs. The ratios of $A\beta_{42/43}$ to total Aβ produced in these experiments were comparable to those produced in PS-null MEFs infected with the corresponding full-length cDNA (Fig. 3*C*). These results confirm that γ-secretase activity was modified by the specific amino acid substitution rather than due to the lack of endoproteolysis of the mutant holoprotein.

R278I mutation does not alter subcellular localization of PS1 protein - Previous studies have suggested that $A\beta_{40}$ and $A\beta_{42/43}$ arise from γ-secretase cleavage at distinct subcellular locations (26-28). However, three observations argue that simple mistrafficking of the $PS1^{LA}$ mutants is not the reason for $A\beta_{42/43}$ production. First, there were no significant differences in the subcellular distribution of WT-PS1 CTF and R278I-PS1 holoprotein in immunocytochemical experiments or upon subcellular fractionation with sucrose gradients (Fig. 4*A* and *B*). Both PS1 species appeared to be similarly transported from the ER to the Golgi apparatus. Second, the pattern of Nct glycosylation in R278I-PS1-expressing cells was indistinguishable from that in WT-PS1-expressing cells (Fig. 4*C*). Finally, the selective over-production of $A\beta_{42/43}$ by R278I- or L435H-PS1 cells was still evident even when Aβ peptides were generated in a solubilized membrane fraction prepared from these cells (Fig. 4*D*).

Different amino acid substitutions at the same residue can result in distinct modifications of γ-secretase activity - The PS1 R278I mutation conferred exclusive generation of $A\beta_{43}$, whereas the P433L mutation resulted in loss-of-function. To address whether these substitutions have a specific role in PS1 endoproteolysis and γ-secretase activities, we generated and tested additional mutations at these residues. We introduced five other mutations into the R278 codon, including FAD-linked R278K and R278T as well as substitutions to S, E, and P, which have polar, negatively charged, and imino group side chains, respectively. Unlike the R278I mutation, all of these substitutions increased the levels of secreted $A\beta_{42/43}$, but did not affect either PS1 endoproteolysis or $A\beta_{40}$ secretion (Fig. 5*A*).

Next we generated seven mutations at the P433 residue and tested γ-secretase activity (Fig. 5*B*). Similar to P433L-PS1, mutant PS1 bearing substitution of P433 with I, E, K, or Q was not cleaved and could not restore Aβ secretion when expressed in PS-null MEFs. In contrast, but similar to $PS1^{LA}$ mutations, the P433S and P433G mutations caused impaired self-endoproteolysis, reduced $A\beta_{40}$ secretion and enhanced $A\beta_{42/43}$ generation. Finally, like FAD-linked mutants, P433A-PS1 was cleaved normally and exhibited a high ratio of $A\beta_{42/43}$ to total Aβ. A434C and L435F, FAD-linked mutations at the neighboring residues of P433, caused enhanced secretion of $A\beta_{42/43}$ (data not shown), and, very recently, A434D and L435R were reported to be loss-of-function mutations (25). Altogether, these results indicate that different amino acid substitutions at the same residue can result in distinct modifications of γ-secretase activity.

Pharmacological assessment of $PS1^{LA}$ mutant-associated protease activities - In addition to mutations of PSs and APP, γ-secretase inhibitors are also known to modulate the ratio of $A\beta_{42/43}$ to total Aβ (29-31). Previous reports have shown that FAD-linked mutations attenuate the effect of γ-secretase inhibitors (32-34); however, these data were obtained from cells expressing both WT and mutant PS1. We therefore re-evaluated the effects of γ-secretase inhibitors using MEFs expressing a single genotype of PS1. The results in Fig. 6*A* confirm

previous reports (30, 35, 36) and show that, in MEFs expressing WT-PS1, the peptidomimetic difluoroketone inhibitor DFK167 selectively enhanced the γ-secretase activity of $A\beta_{42/43}$ generation (γ-42/43) at sub-inhibitory doses, but inhibited the γ-secretase activity of $A\beta_{40}$ generation (γ-40) in a dose-dependent manner. However, this enhancement of $A\beta_{42/43}$ secretion was abolished in MEFs expressing R278I-PSI, and in agreement with the prior report (33), was relatively attenuated in FAD-linked I143F-PS1 MEFs as compared with WT-PS1 MEFs (maximum-fold increases: 0.96 ± 0.01, 1.76 ± 0.08, and 2.06 ± 0.14, respectively; means ± s.d. [n = 3]; $p < 0.001$ by Bonferroni *post-hoc* test).

Sulindac sulfide, a non-steroidal anti-inflammatory drug (NSAID), preferentially inhibits γ-42/43 activity (31, 34, 37, 38). Fig. 6*B* shows that this inhibitory effect was obviously reduced in R278I-PS1MEFs and was intermediately decreased in I143F-PS1 MEFs as compared to WT-PS1 MEFs (fold decreases at 60 μM: 0.96 ± 0.08, 0.49 ± 0.01, and 0.12 ± 0.08, respectively; means ± s.d. [n = 3]; $p < 0.001$ by Bonferroni *post-hoc* test). Paradoxically, $A\beta_{40}$ secretion was enhanced by sulindac sulfide in R278I-PS1 MEFs (maximal fold increase: 3.30 ± 0.28; mean ± s.d. [n = 3]). The inhibition profile of DFK167 or sulindac sulfide in L435H-PS1 MEFs was similar to that of R278I-PS1 (data not shown). Based on these results, it appears that DFK167 and sulindac sulfide have opposite effects; specifically, DFK167 preferentially inhibited γ-40 of $PS1^{LA}$ cells and enhanced γ-42/43 in WT-PS1 cells, whereas sulindac sulfide paradoxically enhanced γ-40 of $PS1^{LA}$ cells and inhibited γ-42/43 in WT-PS1 cells. These results suggest an incomplete reciprocal relationship between γ-40 and γ-42/43 activities. Additionally, it appears that $PS1^{LA}$ mutations cause similar but exaggerated modification on Aβ secretion as compared to FAD-linked mutations.

It has been reported that DFK167 inhibits PS1 endoproteolysis in an *in vitro* assay system (39). However, when DFK167 was applied to cells expressing WT-PS1 or FAD-linked I143F-PS1, the endoproteolysis was unaffected (Fig. 6*C*). Unexpectedly, when DFK167 was applied to cells expressing the R278I- or L435H-PS1 mutant, the endoproteolysis was activated in a dose-dependent manner (Fig. 6*C*). This paradoxical activation was highly specific to these mutants; DFK167 had no effect on the failed endoproteolysis of loss-of-function mutants such as D385A- or P433L-PS1.

DISCUSSION

In this study, we found six missense mutations of PS1 by a random mutagenesis screen for PS1-endoproteolysis-impaired mutants. These mutations fell into two categories: $PS1^{LA}$ and the loss-of-function mutant P433L-PS1. These mutations did not significantly affect the complex assembly and stabilization of uncleaved mutant holoproteins. PSase cleavage is tightly related to γ-secretase activity, although PS endoproteolysis is not absolutely required for the activation of γ-secretase (12, 40). Both activities required two intramembranous aspartyl residues at the putative catalytic sites of PS (D257 and D385 of PS1) (12), and certain γ-secretase inhibitors blocked PSase cleavage as well (41, 42). However, the profiles of their response to inhibitors were different from one another (39, 41). Additionally, a recent report proved that D257A- or D385A-PS1 holoprotein was cleaved, although with low efficiency, without any concomitant γ-secretase activity, when stably expressed in PS-null cells (43). Nevertheless, in most cases,

except mutants harboring mutations at the cleavage site (e.g. M292D-PS1) (40, 44, 45), the previously reported cleavage-defective mutations simultaneously conferred definitive modification of γ-secretase activity and/or specificity (12, 16, 17, 25, 46). This is the case for $PS1^{LA}$ mutants, which are distinctive in mediating exclusively γ-43 cleavage of APP but not self-endoproteolysis, γ-40 and ε-cleavage. $Aβ_{43}$ is a minor Aβ product of normal γ-secretase activity but the longest identified so far, and its secretion, like $Aβ_{42}$, is associated with pathogenic PS1 mutations (33) or DFK167 treatment (36).

Together with previous work, our results suggest that PS mutations allow the existence of at least four activity states of γ-secretase. The lowest activity state is exemplified by loss-of-function mutations such as D257A, D385A, G384K and P433L (12, 16, 17). The next lowest active state is typified by the $PS1^{LA}$ mutants, in which there is residual self-endoproteolysis, γ-40 and ε-cleavage, but relatively high γ-42/43 activity. A further stage of activation, generally supporting normal self-endoproteolysis and γ-40 activity but reduced ε-cleavage and enhanced γ-42/43 activity, is represented by many FAD mutants (5, 18, 33). Finally, WT-PS1 represents the fully functional state, wherein PS1 supports self-endoproteolysis, ε-cleavage, predominant γ-40 activity, and minor γ-42/43 activity. A few FAD mutants have been reported to show reduced self-endoproteolysis and decreased $Aβ_{40}$ secretion as well as enhanced $Aβ_{42/43}$ secretion (41, 47), which somewhat resemble the activity state of $PS1^{LA}$ mutants. Meanwhile, during preparation of this manuscript, R278I $PS1^{LA}$ mutation has been reported to co-segregate with family members affected with early-onset, atypical FAD (48). These suggest that $PS1^{LA}$ mutants have similar but exaggerated effects on γ-secretase activity as compared to typical FAD mutants. PS1 mutations appear to result in a wide spectrum of γ-secretase activity that is associated with a shift in cleavage specificity.

Two of the five $PS1^{LA}$ mutations and the P433L loss-of-function mutation were clustered at the highly conserved PAL sequence in the C-terminal tail. The R278 residue is remote on the sequence from, but can be located close to the PAL motif near the cytoplasmic face of the membrane on the tertiary conformation based on the eight-TM model of PS1 proteins (Fig. 1*B*; 49). These residues may compose of a conformational domain that is important not only for the activity but also for the cleavage specificity of γ-secretase. However, the two other mutations S141R and T245I, which had a weaker effect, were not located in close proximity, suggesting that multiple domains can affect the γ-secretase activity and specificity. On the other hand, our results indicate that different amino acid substitutions at the same residue of PS1 can cause distinct modifications of γ-secretase activity. These results confirm and extend previous studies showing that several mutations at residue 166 or 384 differentially affect secreted Aβ level and the $Aβ_{42}$/total Aβ ratio (16, 18). These observations suggest that the effect of PS mutations on the γ-secretase activity and specificity is not mediated by simple loss of function of a restricted domain or motif.

Recent studies suggest that γ-secretase complexes contain dimerized PS1 or PS2 and that two interfaces with diaspartyl combination in the TM region form catalytic sites (47). Non-competitive inhibition by the transition state analogue inhibitors further indicates that the catalytic sites of γ-secretase are separated from the substrate-docking site(s) (50). Our mutagenesis

study identified no restricted domain responsible for the cleavage specificity. Rather, our results imply that the mutational effects are dependent not only on its position but also on substituting amino acids. Additionally, the effects of $PS1^{LA}$ mutations were accomplished without obvious changes in the composition or subcellular localization of the PS1 complex. These results are consistent with the hypothesis that the γ-secretase complex may have several conformational states linked to distinct γ-secretase activity and specificity. Speculatively, as a result of subtle conformational change by $PS1^{LA}$ or FAD-linked missense mutations, substrates are presented in an aberrant position relative to the catalytic site, causing preferential cleavage at residue 42/43. This effect must be subtle and highly specific, because different amino acid substitutions at the same residues in PS1 cause distinct modifications on γ-secretase activity.

DFK167 and sulindac sulfide are thought to shift the predominant cleavage site, probably through allosteric effects induced by direct PS binding (38, 47, 50, 51). Several of our observations suggest that the effects of PS1 mutations and the allosteric effects of γ-secretase inhibitors are likely to be tightly related, and we speculate that these effects might even be mediated by a shared mechanism. First, our results and previously published data (32-34) show that PS1 mutations clearly modify the response of γ-secretase to these inhibitors. Second, γ-42/43 cleavage enhanced by $PS1^{LA}$ mutations was not further augmented by DFK167 treatment, suggesting that the effect of PS1 mutations and DFK167 treatment on $A\beta_{42/43}$ upregulation share the common plateau level. Third, similar to the case of γ-secretase inhibitor effect, the effect of PS1 mutations on γ-42/43 cleavage is distinct from that on γ-40 and ε-cleavage. Fourth, the paradoxical effect of γ-secretase inhibitors can recover the activities that are inactivated by PS1 mutations. For examples, DFK167 activates endoproteolysis of $PS1^{LA}$ holoproteins and activates γ-42/43 cleavage by WT-PS1, whereas sulindac sulfide activates the γ-40 cleavage which is suppressed by $PS1^{LA}$ mutations.

Taking these observations together, we speculate that various missense mutations of PS1 and the allosteric effects of γ-secretase inhibitors could modulate the cleavage specificity of γ-secretase by the same mechanism, namely a conformational change in the complex. Very recent pharmacological or indirect morphological assessment also indicates that NSAIDs alter PS1 conformation (51, 52). Further, our results suggest a possible reciprocal relationship between γ-40 and γ-42/43 activities. Taken together, these results also suggest that small molecules could be designed to induce alternate PS complex conformations that are more favorable to the generation of $A\beta_{40}$ rather than pathogenic $A\beta_{42/43}$. Such a strategy would obviate the complications of current γ-secretase inhibitor strategies that block all PS-dependent cleavage, including the cleavage of biologically important molecules like the Notch receptors.

REFERENCES

1. Haass, C., and Steiner, H. (2002) *Trends Cell Biol*. **12**, 556-562
2. De Strooper, B. (2003) *Neuron* **38**, 9-12
3. Brown, M.S., Ye, J., Rawson, R.B., and Goldstein, J.L. (2000) *Cell* **100**: 391-398

4. Wang, R., Sweeney, D., Gandy, S.E., and Sisodia, S.S. (1996) *J. Biol. Chem.* **271**, 31894-31902
5. Chen, F., Gu, Y., Hasegawa, H., Ruan, X., Arawaka, S., Fraser, P., Westaway, D., Mount, H., and St George-Hyslop, P. (2002) *J. Biol. Chem.* **277**, 36521-36526
6. Selkoe, D.J. (2002) *J. Clin. Invest.* **110**, 1375-1381
7. Wolfe, M.S., and Haass, C. (2001) *J. Biol. Chem.* **276**, 5413-5416
8. Thinakaran, G., Borchelt, D.R., Lee, M.K., Slunt, H.H., Spitzer, L., Kim, G., Ratovitsky, T., Davenport, F., Nordstedt, C., Seeger, M., Hardy, J., Levey, A.I., Gandy, S.E., Jenkins, N.A., Copeland, N.G., Price, D.L., and Sisodia, S.S. (1996) *Neuron* **17**, 181-190
9. Podlisny, M.B., Citron, M., Amarante, P., Sherrington, R., Xia, W., Zhang, J., Diehl, T., Levesque, G., Fraser, P., Haass, C., Koo, E.H., Seubert, P., St George-Hyslop, P., Teplow, D.B., and Selkoe, D.J. (1997) *Neurobiol. Dis*. **3**, 325-337
10. Yu, G., Nishimura, M., Arawaka, S., Levitan, D., Zhang, L., Tandon, A., Song, Y.Q., Rogaeva, E., Chen, F., Kawarai, T., Supala, A., Levesque, L., Yu, H., Yang, D.S., Holmes, E., Milman, P., Liang, Y., Zhang, D.M., Xu, D.H., Sato, C., Rogaev, E., Smith, M., Janus, C., Zhang, Y., Aebersold, R., Farrer, L.S., Sorbi, S., Bruni, A., Fraser, P., and St George-Hyslop, P. (2000) *Nature* **407**, 48-54
11. Francis, R., McGrath, G., Zhang, J., Ruddy, D.A., Sym, M., Apfeld, J., Nicoll, M., Maxwell, M., Hai, B., Ellis, M.C., Parks, A.L., Xu, W., Li, J., Gurney, M., Myers, R.L., Himes, C.S., Hiebsch, R., Ruble, C., Nye, J.S., and Curtis, D. (2002) *Dev. Cell* **3**, 85-97
12. Wolfe, M.S., Xia, W., Ostaszewski, B.L., Diehl, T.S., Kimberly, W.T., and Selkoe, D.J. (1999) *Nature* **398**, 513-517
13. Li, Y.M., Xu, M., Lai, M.T., Huang, Q., Castro, J.L., DiMuzio-Mower, J., Harrison, T., Lellis, C,. Nadin, A., Neduvelil, J.G., Register, R.B., Sardana, M.K., Shearman, M.S., Smith, A.L., Shi, X.P., Yin, K.C., Shafer, J.A., and Gardell, S.J. (2000) *Nature* **405**, 689-694
14. Takasugi, N., Tomita, T., Hayashi, I., Tsuruoka, M., Niimura, M., Takahashi, Y., Thinakaran, G., and Iwatsubo, T. (2003) *Nature* **422,** 438-441
15. Edbauer, D., Winkler, E., Regula, J.T., Pesold, B., Steiner, H., and Haass, C. (2003*) Nat. Cell Biol.* **5**, 486-488
16. Steiner, H., Kostka, M., Romig, H., Basset, G., Pesold, B., Hardy, J., Capell, A., Meyn, L., Grim, M.L., Baumeister, R., Fechteler, K., and Haass, C. (2000) *Nat. Cell Biol.* **2**, 848-851
17. Tomita, T., Watabiki, T., Takikawa, R., Morohashi, Y., Takasugi, N., Kopan, R., De Strooper, B., and Iwatsubo, T. (2001) *J. Biol. Chem.* **276**, 33273-33281
18. Moehlmann, T., Winkler, E., Xia, X., Edbauer, D., Murrell, J., Capell, A., Kaether, C., Zheng, H., Ghetti, B., Haass, C., and Steiner, H. (2002) *Proc. Natl. Acad. Sci. USA* **99**, 8025-8030
19. Wrigley, J.D., Nunn, E.J., Nyabi, O., Clarke, E.E., Hunt, P., Nadin, A., De Strooper, B., Shearman, M.S., and Beher, D. (2004) *J. Neurochem.* **90**, 1312-1320
20. Herreman, A., Serneels, L., Annaert, W., Collen, D., Schoonjans, L., and De Strooper, B. (2002) *Nat. Cell Biol.* **2**, 461-462
21. Kitamura, T., Onishi, M., Kinoshita, S., Shibuya, A., Miyajima, A., and Nolan, G.P. (1995) *Proc. Natl. Acad. Sci. USA* **92**, 9146-9150
22. Yu, G., Chen, F., Levesque, G., Nishimura, M., Zhang, D.M., Levesque, L., Rogaeva, E., Xu, D.,

Liang, Y., Duthie, M., St George-Hyslop, P.H., and Fraser, P.E. (1998) *J. Biol. Chem.* **273**, 16470-16475

23. Schroeter, E.H., Kisskinger, J.A., and Kopan, R. (1998) *Nature* **393**, 382-386
24. Komano, H., Shiraishi, H., Kawamura, Y., Sai, X., Suzuki, R., Serneels, L., Kawaichi, M., Kitamura, T., and Yanagisawa, K. (2002) *J. Biol. Chem.* **277**, 39627-39633
25. Wang, J., Brunkan, A.L., Hecimovic, S., Walker, E., and Goate, A. (2004) *Neurobiol. Dis.* **15**, 654-666
26. Hartmann, T., Bieger, S.C., Bruhl, B., Tienari, P.J., Ida, N., Allsop, D., Roberts, G.W., Masters, C.L., Dotti, C.G., Unsicker, K., and Beyreuther, K. (1997) *Nat. Med.* **3**, 1016-1020
27. Cook, D.G., Forman, M.S., Sung, J.C., Leight, S., Kolson, D.L., Iwatsubo, T., Lee, V.M., and Doms, R.W. (1997) *Nat. Med.* **3**, 1021-1023
28. Greenfield, J.P., Tsai, J., Gouras, G.K., Hai, B., Thinakaran, G., Checler, F., Sisodia, S.S., Greengard, P., and Xu, H. (1999) *Proc. Natl. Acad. Sci. USA* **96**, 742-747
29. Citron, M., Diehl, T.S., Gordon, G., Biere, A.L., Seubert, P., and Selkoe, D.J. (1996) *Proc. Natl. Acad. Sci. USA* **93**, 13170-13175
30. Zhang, L., Song, L., Terracina, G., Liu, Y., Pramanik, B., and Parker, E. (2001) *Biochemistry* **40**, 5049-5055
31. Weggen, S., Eriksen, J.L., Das, P., Sagi, S.A., Wang, R., Pietrzik, C.U., Findlay, K.A., Smith, T.E., Murphy, M.P., Bulter, T., Kang, D.E., Marquez-Sterling, N., Golde, T.E., and Koo, E.H. (2001) *Nature* **414**, 212-216
32. Xia, W., Ostaszewski, B.L., Kimberly, W.T., Rahmati, T., Moore, C.L., Wolfe, M.S., and Selkoe, D.J. (2000) *Neurobiol. Dis.* **7**, 673-681
33. Ikeuchi, T., Dolios, G., Kim, S.H., Wang, R., and Sisodia, S.S. (2003) *J. Biol. Chem.* **278**, 7010-7018
34. Weggen, S., Eriksen, J.L., Sagi, S.A., Pietrzik, C.U., Ozols, V., Fauq, A., Golde, T.E., and Koo, E.H. (2003) *J. Biol. Chem.* **278**, 31831-31837
35. Wolfe, M.S., Xia, W., Moore, C.L., Leatherwood, D.D., Ostaszewski, B., Rahmati, T., Donkor, I.O., and Selkoe, D.J. (1999) *Biochemistry* **38**, 4720-4727
36. Beher, D., Wrigley, J.D., Owens, A.P., and Shearman, M.S. (2002) *J. Neurochem.* **82**, 563-575
37. Takahashi, Y., Hayashi, I., Tominari, Y., Rikimaru, K., Morohashi, Y., Kan, T., Natsugari, H., Fukuyama, T., Tomita, T., and Iwatsubo, T. (2003) *J. Biol. Chem.* **278**, 18664-18670
38. Beher, D., Clarke, E.E., Wrigley, J.D., Martin, A.C., Nadin, A., Churcher, I., and Shearman, M.S. (2004) *J. Biol. Chem.* **279**, 43419-43426
39. Campbell, W.A., Reed, M.L., Strahle, J., Wolfe, M.S., and Xia, W. (2003) *J. Neurochem.* **85**, 1563-1574
40. Steiner, H., Romig, H., Pesold, B., Philipp, U., Baader, M., Citron, M., Loetscher, H., Jacobsen, H., and Haass, C. (1999) *Biochemistry* **38**, 14600-14605
41. Beher, D., Wrigley, J.D., Nadin, A., Evin, G., Masters, C.L., Harrison, T., Castro, J.L., and Shearman, M.S. (2001) *J. Biol. Chem.* **276**, 45394-45402
42. Campbell, W.A., Iskandar, M.K., Reed, M.L., and Xia, W. (2002) *Biochemistry* **41**, 3372-3379
43. Nyabi, O., Bentahir, M., Horre, K., Herreman, A., Gottardi-Littell, N., Van Broeckhoven, C.,

Merchiers, P., Spittaels, K., Annaert, W., and De Strooper, B. (2003) *J. Biol. Chem.* **278**, 43430-43436
44. Jacobsen, H., Reinhardt, D., Brockhaus, M., Bur, D., Kocyba, C., Kurt, H., Grim, M.G., Baumeister, R., and Loetscher, H. (1999) *J. Biol. Chem.* **274**, 35233-35239
45. Shirotani, K., Takahashi, K., Araki, W., Maruyama, K., and Tabira, T. (2000) *J. Biol. Chem.* **275**, 3681-3686
46. Mercken, M., Takahashi, H., Honda, T., Sato, K., Murayama, M., Nakazato, Y., Noguchi, K., Imahori, K., and Takashima, A. (1996) *FEBS Lett.* **389**, 297-303
47. Schroeter, E.H., Ilagan, M.X., Brunkan, A.L., Hecimovic, S., Li, Y.M., Xu, M., Lewis, H.D., Saxena, M.T., De Strooper, B., Coonrod, A., Tomita, T., Iwatsubo, T., Moore, C.L., Goate, A., Wolfe, M.S., Shearman, M., and Kopan, R. (2003) *Proc. Natl. Acad. Sci. USA* **100**, 13075-13080
48. Godbolt, A.K., Beck, J.A., Collinge, J., Garrard, P, Warren, J.D., Fox, N.C., and Rossor, M.N. (2004) *Neurology* **63**, 1702-1704
49. Doan, A., Thinakaran, G., Borchelt, D.R., Slunt, H.H., Ratovitsky, T., Podlisny, M., Selkoe, D.J., Seeger, M., Gandy, S.E., Price, D.L., and Sisodia, S.S. (1996) *Neuron* **17**, 1023-1030
50. Tian, G., Sobotka-Briner, C.D., Zysk, J., Liu, X., Birr, C., Sylvester, M.A., Edwards, P.D., Scott, C.D., and Greenberg, B.D. (2002) *J. Biol. Chem.* **277**, 31499-31505
51. Esler, W.P., Kimberly, W.T., Ostaszewski, B.L., Diehl, T.S., Moore, C.L., Tsai, J.Y., Rahmati, T., Xia, W., Selkoe, D.J., and Wolfe, M.S. (2000) *Nat. Cell Biol.* **2**, 428-434
52. Lleo, A., Berezovska, O., Herl, L., Raju, S., Deng, A., Bacskai, B.J., Frosch, M.P., Irizarry, M., and Hyman, B.T. (2004) *Nat. Med.* **10**, 1065-1066

FOOTNOTES

*We thank Drs. Raphael Kopan and Toshio Kitamura for Notch constructs and retrovirus vector, respectively, and Miwako Nishikawa for technical assistance. We acknowledge the Central Laboratory of the Shiga University of Medical Science for assistance in the DNA sequencing. This work was supported in part by a Grant-in-Aid for Scientific Research from MEXT, Japan (to M.N.), as well as grants from the Life Science Foundation and the Uehara Memorial Foundation (to M.N.), the Canadian Institute of Health Research and Howard Hughes Medical Institute (to P.H.), the Ontario Mental Health Foundation (to P.F.), and NIH (AG10491 to R.W.).

[1]The abbreviations used are: Aβ, amyloid β; APP, amyloid β-precursor protein; AICD, APP intracellular domain; FAD, familial Alzheimer's disease; PS, presenilin; PSase, presenilinase; $PS1^{LA}$, presenilin 1 generating long amyloid β; nicastrin, Nct; NICD, Notch intracellular domain; NTF, N-terminal fragment; CTF, C-terminal fragment; FL, full-length; TM, transmembrane; WT, wild-type; MW, molecular weight; NSAID, non-steroidal anti-inflammatory drug; MEF, mouse embryonic fibroblast; HEK293, human embryonic kidney 293; ELISA, enzyme-linked immunosorbent assay; CHAPSO, 3-[(3-cholamidopropyl)dimethylammonio]-2-hydroxy-1-propanesulfonic acid; IP/MS, immunoprecipitation/mass spectrometry; MALDI-TOF-MS, matrix-assisted laser desorption/ionization time-of-flight mass spectrometry.

FIGURE LEGENDS

Fig. 1. **Endoproteolysis-impaired missense mutant PS1 proteins form stable, high molecular weight complexes.** ***A*,** Impaired endoproteolysis of mutant PS1 proteins. The membrane fraction from PS-null MEFs transiently transfected with each PS1 mutant was immunoblotted with anti-PS1 antibody. WT-PS1 and the loss-of-function mutant, D385A-PS1, served as controls. ***B*,** A scheme showing the location of mutated residues in PS1 mutants on the 8-TM model. ***C*,** Glycerol velocity gradient fractions of CHAPSO lysates from PS1-transfected HEK293 cells were analyzed for PS1. The positions of molecular weight markers are indicated at the top of the panel. Results are representative of three independent experiments. ***D*,** After treatment with 25 μg/ml cycloheximide for the indicated time, the lysate from HEK293 cells stably expressing each PS1 was detected using anti-PS1 antibody.

Fig. 2. **PS-dependent protease activities in mutant PS1-expressing HEK293 cells.** ***A*,** ε-Cleavage in cells stably expressing mutant PS1 and APP-C99. AICD fragments generated from 0.5% CHAPSO-extracted membrane fractions were evaluated by immunoblotting with an anti-APP antibody. WT-PS1 and the loss-of-function mutant, D385A-PS1, served as controls. Results are representative of at least three independent experiments. ***B*,** S3 cleavage of Notch in mutant PS1-expressing cells. After transient transfection with NotchΔE-Myc, mutant PS1-expressing cells were metabolically pulse-labeled and chased for 1 h. Immunoprecipitates with anti-Myc antibody were analyzed by polyacrylamide gel electrophoresis. An autoradiograph of the dried gel is shown. ***C*,** Aβ secretion from cells expressing WT or mutant PS1. $A\beta_{40}$ and $A\beta_{42/43}$ levels in the conditioned media were quantified by ELISA. Data represent the means ± s.d. (n=3). $*p < 0.001$ by one-way ANOVA with Dunnett's *post-hoc* test as compared with the values in WT PS1 cells.

Fig. 3. **γ-Secretase activities of mutant PS1 on a PS-null background.** ***A*,** Aβ secretion from PS-null MEFs transfected with mutant PS1. PS-null MEFs were retrovirally co-transfected with PS1 and APP, and secreted Aβ levels were measured by ELISA. Data represent the means ± s.d. (n = 3). Lower panels show the immunoblots for transfected PS1, APP, and secreted APP ectodomain (s-APP). ***B*,** The profile of Aβ species secreted from PS-null MEFs transfected with WT, R278I- or L435H-PS1 was analyzed using IP/MS. ***C*,** Secreted Aβ levels from PS-null MEFs co-transfected with human APP and indicated PS1 constructs were measured by ELISA. The ratios of $A\beta_{42/43}$ to total Aβ are shown. Data represent the means ± s.d. (n = 3).

Fig. 4. **Subcellular localization of PS1 and cleavage specificity of γ-secretase.** ***A*,** PS-null MEFs retrovirally transfected with WT or R278I-PS1 were investigated by immunocytochemistry. Immunoreactivities for PS1 CTF and the Golgi marker protein, p115, are shown in red and green, respectively. Merged images show localization of PS1 in the Golgi apparatus as yellow fluorescence. ***B*** and ***C*,** HEK293 cells stably transfected with WT or R278I-PS1 were fractionated by sucrose density centrifugation. The fractionated proteins were analyzed by immunoblottting with an anti-PS1 (*B*) or

anti-Nct (*C*) antibody. ***D*,** The Aβ generated in cell-free systems in CHAPSO lysates of membrane fractions from HEK293 cells overexpressing each PS1 was assessed by ELISA. The ratios of $A\beta_{42/43}$ to total Aβ are shown. Data represent the means ± s.d. (n = 3).

Fig. 5. **γ-Secretase activity of PS1 with mutations at residue 278 or 433.** ***A*,** PS1 mutants containing six different substitutions at R278 were transfected into PS-null MEFs. An immunoblot for transfected PS1 is shown in the upper panel. The graph shows Aβ levels in the conditioned media as estimated by ELISA. Values represent the means ± s.d. (n = 3). **p*<0.001 by one-way ANOVA with Dunnett's *post-hoc* test. ***B*,** PS1 mutants containing eight different substitutions at P433 were transfected into PS-null MEFs. Shown is an immunoblot for PS1 (upper panel) and Aβ levels in the conditioned media (graph). Values represent the means ± s.d. (n = 3).

Fig. 6. **Effect of DFK167 and sulindac sulfide on Aβ secretion and PS1 endoproteolysis.** ***A*** and ***B*,** PS-null MEFs co-transfected with human APP and WT-, I143F-, or R278I-PS1 were treated for 12 h with the indicated concentrations of DFK167 or sulindac sulfide, and $A\beta_{40}$ and $A\beta_{42/43}$ in the medium were measured by ELISA. Data represent the means ± s.d. (n = 3). ***C*,** After DFK167 treatment of mutant PS1-expressing MEFs for 12 h, PS1 endoproteolysis was estimated by immunoblotting with an anti-PS1 CTF antibody. The results are representative of three independent experiments.

Figure 1

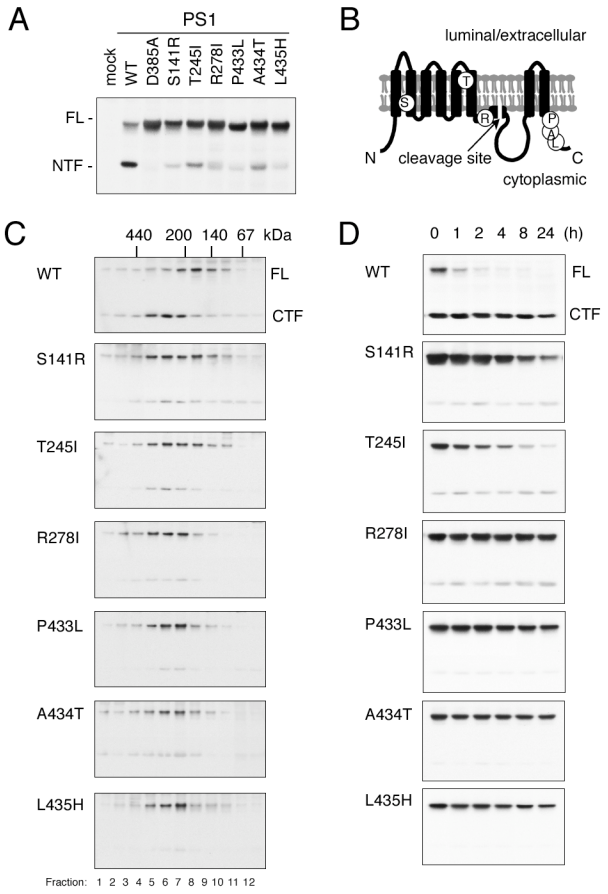
A
PS1
mock
WT
D385A
S141R
T245I
R278I
P433L
A434T
L435H
FL -
NTF -
B
luminal/extracellular
S
T
R
P
A
L
N
cleavage site
C
cytoplasmic
C
440 200 140 67 kDa
WT
FL
CTF
S141R
T245I
R278I
P433L
A434T
L435H
Fraction: 1 2 3 4 5 6 7 8 9 10 11 12
D
0 1 2 4 8 24 (h)
WT
FL
CTF
S141R
T245I
R278I
P433L
A434T
L435H

Figure 2

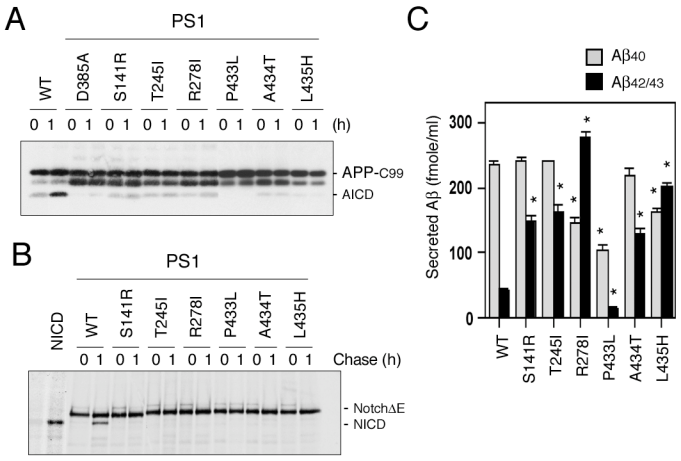
A
PS1
WT
D385A
S141R
T245I
R278I
P433L
A434T
L435H
0 1 0 1 0 1 0 1 0 1 0 1 0 1 0 1 (h)
APP-C99
AICD
B
PS1
NICD
WT
S141R
T245I
R278I
P433L
A434T
L435H
0 1 0 1 0 1 0 1 0 1 0 1 0 1 Chase (h)
NotchΔE
NICD
C
Aβ40
Aβ42/43
Secreted Aβ (fmole/ml)
300
200
100
0
WT
S141R
T245I
R278I
P433L
A434T
L435H

Figure 3

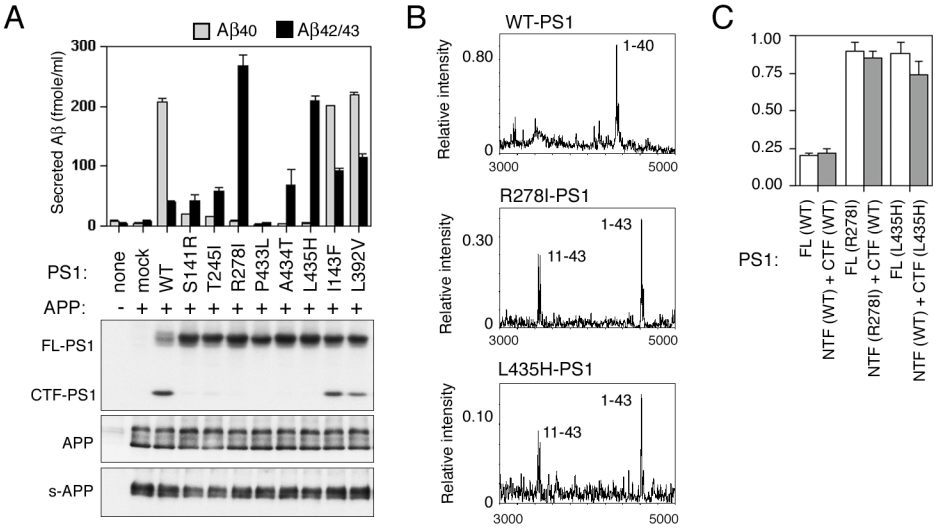
A
Aβ40
Aβ42/43
Secreted Aβ (fmole/ml)
300
200
100
0
PS1:
none
mock
WT
S141R
T245I
R278I
P433L
A434T
L435H
I143F
L392V
APP:
- + + + + + + + + + +
FL-PS1
CTF-PS1
APP
s-APP
B
WT-PS1
1-40
Relative intensity
0.80
0
3000
5000
R278I-PS1
1-43
11-43
0.30
L435H-PS1
0.10
C
1.00
0.75
0.50
0.25
0.00
PS1:
FL (WT)
NTF (WT) + CTF (WT)
FL (R278I)
NTF (R278I) + CTF (WT)
FL (L435H)
NTF (WT) + CTF (L435H)

Figure 4

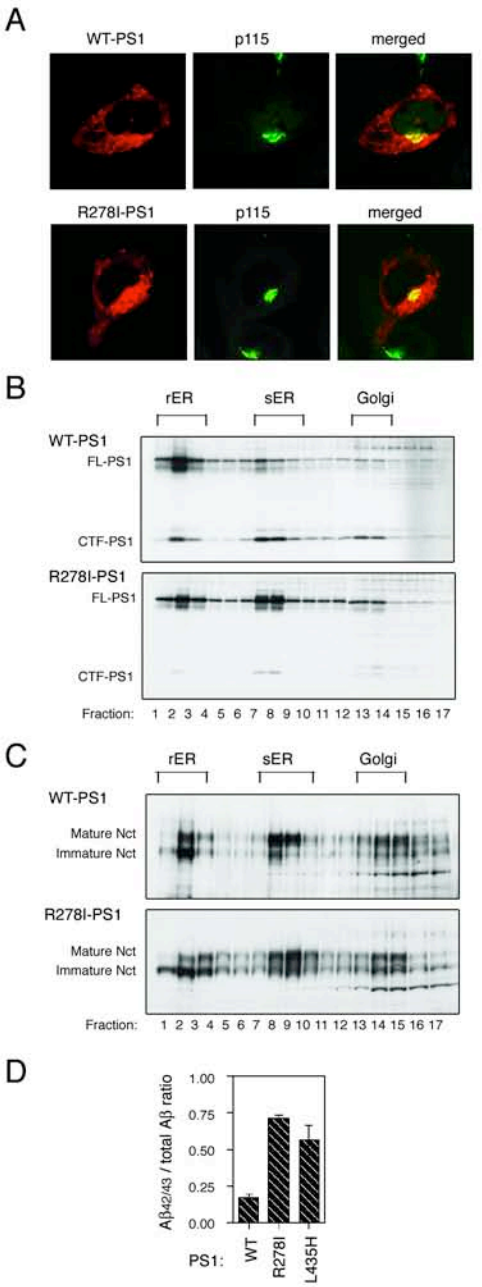
A
WT-PS1
p115
merged
R278I-PS1
p115
merged
B
rER
sER
Golgi
WT-PS1
FL-PS1
CTF-PS1
R278I-PS1
FL-PS1
CTF-PS1
Fraction: 1 2 3 4 5 6 7 8 9 10 11 12 13 14 15 16 17
C
rER
sER
Golgi
WT-PS1
Mature Nct
Immature Nct
R278I-PS1
Mature Nct
Immature Nct
Fraction: 1 2 3 4 5 6 7 8 9 10 11 12 13 14 15 16 17
D
Aβ42/43 / total Aβ ratio
1.00
0.75
0.50
0.25
0.00
PS1:
WT
R278I
L435H

Figure 5

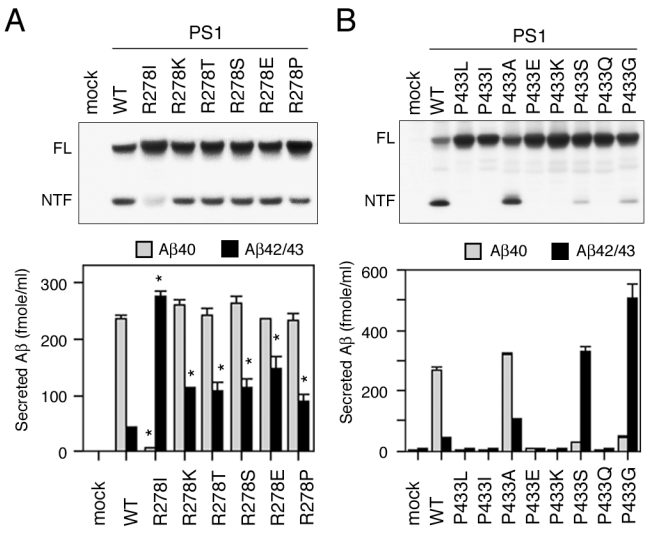
A
PS1
mock
WT
R278I
R278K
R278T
R278S
R278E
R278P
FL
NTF
Aβ40
Aβ42/43
Secreted Aβ (fmole/ml)
300
200
100
0
B
PS1
mock
WT
P433L
P433I
P433A
P433E
P433K
P433S
P433Q
P433G
FL
NTF
Aβ40
Aβ42/43
Secreted Aβ (fmole/ml)
600
400
200
0

Figure 6

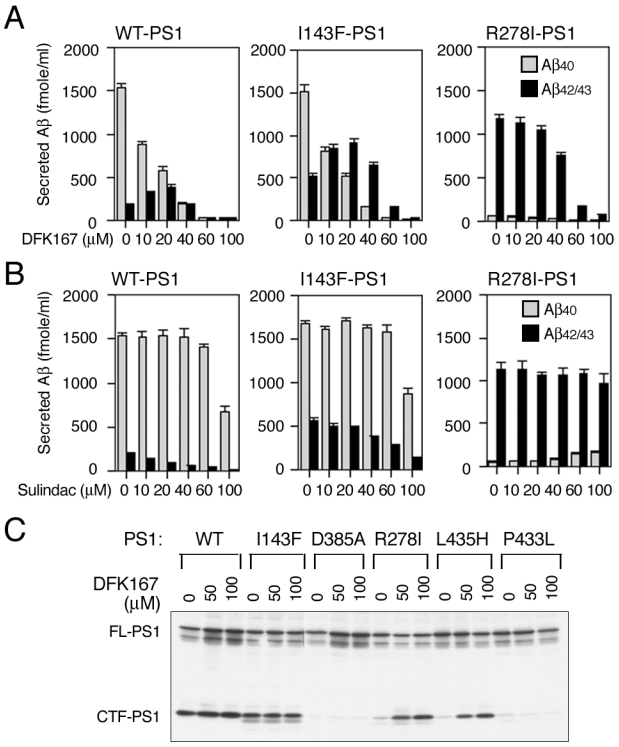
A
WT-PS1
I143F-PS1
R278I-PS1
Secreted Aβ (fmole/ml)
2000
1500
1000
500
0
Aβ40
Aβ42/43
DFK167 (μM) 0 10 20 40 60 100
B
WT-PS1
I143F-PS1
R278I-PS1
Secreted Aβ (fmole/ml)
Aβ40
Aβ42/43
Sulindac (μM) 0 10 20 40 60 100
C
PS1: WT I143F D385A R278I L435H P433L
DFK167 (μM)
0 50 100
FL-PS1
CTF-PS1